

## Impurity band conduction in $\text{FeSi}_{1-x}\text{Al}_x$

This article has been downloaded from IOPscience. Please scroll down to see the full text article.

2008 J. Phys.: Condens. Matter 20 325238

(<http://iopscience.iop.org/0953-8984/20/32/325238>)

View [the table of contents for this issue](#), or go to the [journal homepage](#) for more

Download details:

IP Address: 129.252.86.83

The article was downloaded on 29/05/2010 at 13:49

Please note that [terms and conditions apply](#).

# Impurity band conduction in $\text{FeSi}_{1-x}\text{Al}_x$

L S Sharath Chandra, Archana Lakhani, Mohan Gangrade and V Ganesan

UGC-DAE Consortium for Scientific Research, Khandwa Road, Indore, 452017, Madhya Pradesh, India

E-mail: [vganesan@csr.ernet.in](mailto:vganesan@csr.ernet.in)

Received 27 February 2008, in final form 27 June 2008

Published 21 July 2008

Online at [stacks.iop.org/JPhysCM/20/325238](http://stacks.iop.org/JPhysCM/20/325238)

## Abstract

Precise resistivity and thermopower measurements across the metal insulator transition in Al doped correlated semiconductor FeSi are reported. Doping of carriers results in the emergence of electronic states at the Fermi level. For sufficient concentration of dopant, these states form into an impurity band. The properties of such systems are governed by this impurity band at low temperatures and the semiconducting bands at higher temperatures. Here we show the applicability of such a two-band structure to account for the temperature dependence of resistivity and thermopower in metals near the metal insulator transition.

(Some figures in this article are in colour only in the electronic version)

## 1. Introduction

FeSi is a correlated non-magnetic semiconductor having an energy gap of about 50 meV. It has been attractive among the scientific community for more than three decades due to its unusual magnetic properties [1–5]. Insulator to metal transition is observed for substitution in both sites, Fe [6–9] and Si [10–12]. In the ligand site of Si, hole doping through aluminum leads to a heavy Fermi liquid metal with a critical concentration of  $x_c = 0.005$ . Metal insulator (MI) transition in  $\text{FeSi}_{1-x}\text{Al}_x$  is identified to be similar to Si:P [11, 12]. Mass enhancement of carriers arises from the strong correlations involved. Substitution of carriers into a semiconductor will result in the appearance of electronic states at the Fermi level. As carrier doping increases, these electronic states form into a half filled impurity band leading to an MI transition. The temperature dependence of resistivity  $\rho$  shows a broad peak ( $T_{\rho P}$ ) for metals near MI transition. As concentration of dopant increases,  $T_{\rho P}$  shifts to higher temperatures and vanishes for metals far from the MI transition [11–13]. Below  $T_{\rho P}$ ,  $\rho$  has a positive temperature coefficient corresponding to metallic behavior. While for  $T > T_{\rho P}$  an exponential decrease in  $\rho$  is observed. Similarly thermopower  $S$  also shows a peak ( $T_{SP}$ ) in its temperature dependence. Below  $T_{SP}$ ,  $S$  has a linear temperature dependence, while above  $T_{SP}$ ,  $S$  decreases as  $T^{-1}$ . The temperature dependence of  $\rho$  and  $S$  may be represented by a metal in parallel with that for a semiconductor. This two-band or parallel-resistor model was extensively used in describing high temperature superconductors [14] as well as

Kondo semiconductor/semimetal CeNiSn [15]. However, such a quantitative attempt for metals derived by MI transition has not been reported in the literature.

In this paper, we report resistivity and thermopower measurements on Al doped FeSi across the MI transition. The temperature dependences of  $\rho$  and  $S$  in doped samples are described on the basis the model mentioned above.

## 2. Experimental details

Polycrystalline samples were prepared by taking elements of purity better than 99.95%. Ingredients in stoichiometric proportions were melted in an argon arc furnace. Ingots thus formed were drawn into rectangular rods. Samples were annealed in evacuated quartz ampoules at 1000 °C for one week to increase the homogeneity and to relieve strain. X-ray diffraction measurements were carried out using a Rigaku diffractometer with Cu K $\alpha$  radiation. The absence of impurity peaks reveals that the samples were formed in a single phase. Resistivity measurements were carried out down to 2 K in the four probe configuration. Thermopower measurements were carried out by the differential sandwich method using a closed cycle refrigerator in the temperature range of 4–300 K with an in-house developed platform.

## 3. Results

Resistivity measurements down to 2 K are shown in figure 1. For FeSi, resistivity increases by four orders of magnitude

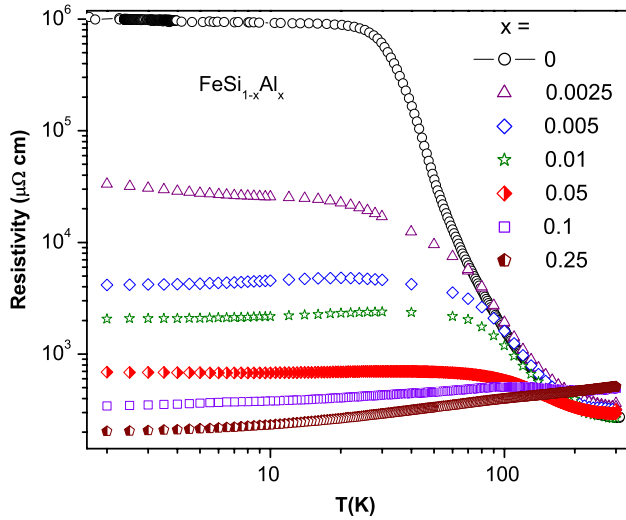


**Figure 1.** Resistivity measurements down to 2 K for  $x = 0$ – $0.25$  in  $\text{FeSi}_{1-x}\text{Al}_x$ .

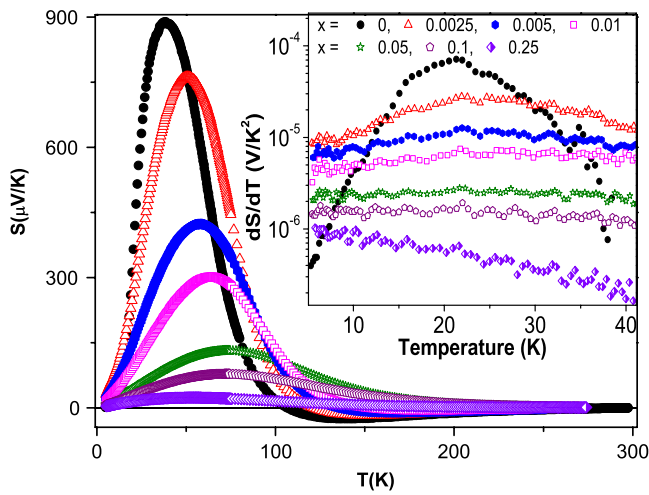


**Figure 2.** Thermopower of Al doped FeSi up to  $x = 0.25$ . As the concentration of carriers increases, the absolute thermopower at low temperatures decreases. High temperature negative thermopower becomes positive as Al concentration increases due to hole doping. (Inset)  $dS/dT$  showing linear  $S$  below 40 K for doped samples.

upon cooling from 300 to 2 K. Activated behavior is observed in the temperature range of 30–200 K with an activation energy  $\approx 640$  K. Slope change below 30 K is attributed to extrinsic conduction through variable range hopping. Resistivity is substantially reduced by a small amount of Al substitution. MI transition occurs for  $x_c = 0.005$  which is on a par with the literature value [11, 12]. For  $x = x_c$ , a peak in resistivity is observed at  $T_{\rho P} = 20$  K. As aluminum concentration increases,  $T_{\rho P}$  shifts to high temperatures. For  $x = 0.1$ ,  $T_{\rho P} = 107$  K and vanishes for  $x = 0.25$  (figure 3).

The thermopower down to  $\approx 4$  K is shown in figure 2. At 300 K,  $S$  for all the samples is very small, of the order of  $1 \mu\text{V K}^{-1}$  or less. For FeSi, thermopower becomes negative when the temperature is decreased below 290 K. A negative peak of  $25 \mu\text{V K}^{-1}$  is observed at 150 K. The manifestation of a gap in the density of states below 200 K results in a large

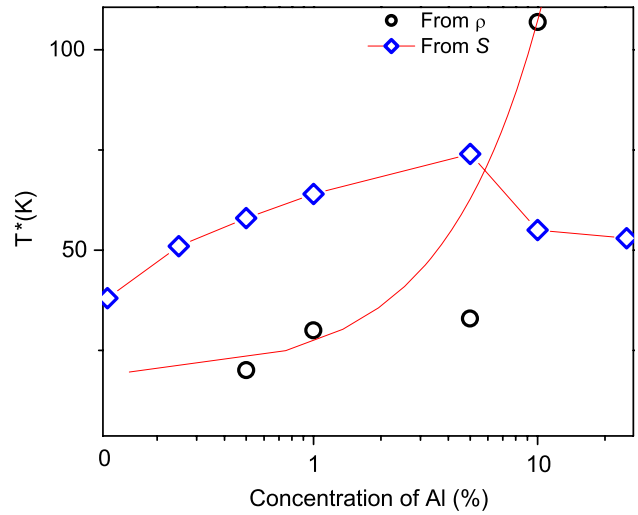


**Figure 3.** The temperature corresponding to the peak in resistivity and thermopower as a function of Al concentration. The peak shifts to higher temperature as concentration is increased. For the resistivity, the peak vanishes for  $x = 0.25$ . However, for thermopower we find a peak for  $x = 0.25$ .

positive peak at 35 K (figure 2). This low temperature peak may have an origin either from the phonon drag mechanism [6] or the correlations which makes  $S$  become zero [16]. As aluminum concentration increases,  $S$  above 150 K become more positive as compared to FeSi. For concentrations of 5% and above,  $S$  is positive over our temperature range of measurements. At low temperatures, a linear temperature dependence of  $S$  is observed. This is indicated by constant  $dS/dT$  (inset of figure 2). A huge increase in  $S$  at 5 K for a small amount of Al doping is observed. Again,  $S$  decreases for an increased amount of Al doping. It is to be noted that the FeSi has the lowest value of  $S$  at 5 K. Thus, the observed features are due to an increase in the number of carriers at the Fermi level resulting in a decrease of contributions from the phonon drag mechanism [17]. In figure 3, we show the temperature  $T_{SP}$  as a function of Al concentration along with  $T_{\rho P}$ . The peak shifts to high temperature as Al concentration increases and then decreases to lower temperatures for  $x \geq 0.1$

## 4. Discussion

### 4.1. Description of the model

For a two-band conduction, the effective conductivity is given by

$$\sigma = \sigma_1 + \sigma_2 = 1/\rho. \quad (1)$$

The contributions from different bands add as the resistors are in a parallel configuration. The  $\sigma_1$  is from the metallic impurity band. For simplicity, we assume the linear temperature dependence of resistivity for this band as  $\sigma_1 = (\sigma_{01}^{-1} + aT)^{-1}$ .  $\sigma_2$  is the activated conduction from semiconducting bands as  $\sigma_2 = \sigma_{02} \exp(-E_g/2k_B T)$ , where  $E_g$  is the activation energy and  $k_B$  is the Boltzmann constant.

Thermopower for this configuration is derived using the Nordheim–Gorter rule [18] as

$$S = (S_1\sigma_1 + S_2\sigma_2)/(\sigma_1 + \sigma_2) \quad (2)$$

**Table 1.** Parameters of fitting of resistivity and thermopower using equations (1) and (2), respectively.

Concentration (%)	$1/\sigma_{01}$ ( $\mu\Omega$ cm)	$a$ ( $\mu\Omega$ cm $K^{-1}$ )	$1/\sigma_{02}$ ( $\mu\Omega$ cm)	$E_{g\rho}$ (K)	$A$ ( $\mu V K^{-2}$ )	$C$ ( $\mu V K^{-1}$ )	$E_{gS}$ (K)
1	2323	0.913	0.02466	810	5.597	-347.4	813
5	687	0.249	0.00892	666	2.315	-425.7	645
10	367	1.908	0.00385	616	1.479	-375	475
25	199	3.367	0.00152	163	0.742	-204.6	209

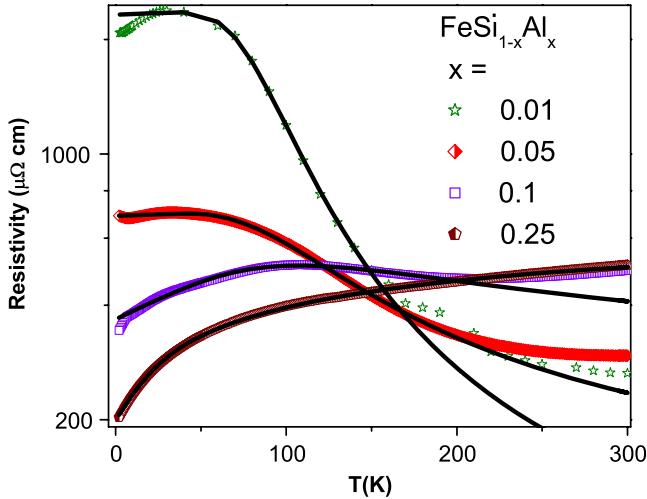


**Figure 4.** Resistivity for  $x > x_c$  is fitted using equation (1). The fit improves over a larger temperature range at higher concentration due to the well formed impurity band. The parameters are tabulated in table 1.

where  $S_1 = AT = \pi^2 k_B^2 T / 2e E_F$  is the diffusion thermopower for metals and  $S_2$  is the thermopower for semiconductors.  $S_2 = C + 8.61 E_g / T$  is for the present case [16]. For metals far from the MI transition, one can use the simplified version of this equation [14].

At low temperatures, as activated carriers freeze out, the conductivity is dominated by the impurity band, leading to a positive coefficient of resistivity and a linear thermopower. At high temperatures, electrons at the valence band will gain sufficient energy to jump into the conduction band and these activated carries dominate the conductivity. Hence, an exponential decrease in resistivity and an inverse temperature dependence of thermopower are the expected outcomes.

#### 4.2. Two-band description for $FeSi_{1-x}Al_x$

Doping of Al in FeSi introduces holes at the Fermi level. In the semiconducting regime, i.e. for  $x < x_c$ , the electronic states will be localized and the hopping conduction will dominate. In such cases, it is not possible to fit the resistivity by equation (1). However, for  $x > x_c$  the electronic states will form into a band. Then the conductivity at low temperature is dominated by this band leading to a metallic behavior. The resistivity for samples with  $x = 0.01-0.25$  is plotted in figure 4. The solid line represents the fit using equation (1). The parameters of the fit are given in table 1. At low concentration of Al, the temperature dependence of metallic conductivity is negligibly

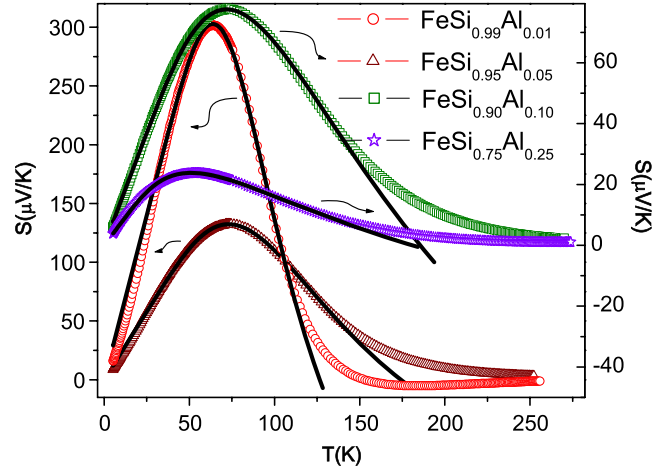


**Figure 5.** Two-band model of thermopower of Al concentration  $x = 0.01, 0.05$  and  $0.1$  and  $0.25$ . The open circles are the experimental data points and the solid line represents the fit using equation (2).

small. The scattering from this band acts as a background resistivity  $\rho_{01} = 1/\sigma_{01}$  over which semiconducting behavior is seen. However, below 20 K there is a drop in resistivity for  $x = 0.01$  which cannot be accounted for by this model. This is due to the assumption of linear resistivity for the metallic band. The resistivity of metals close to MI transition has a different temperature dependence than that assumed, and hence deviations are observed for this composition. Again, at high temperatures, the fit deviates from the parallel-resistor model due to the closure of the activation gap. As concentration of Al increases, the coefficient  $a$  of the metallic contribution increases and the gap value decreases. Hence, the fitting is applicable below 200 K for  $x \leq 0.1$ . However, at  $x = 0.25$ , metallic contribution dominates with resistivity similar to metals like Cu, hence our assumption of  $\sigma_{01}$  is true over the entire temperature range.

In the case of heavily doped semiconductors or metals near the metal insulator transition, the temperature dependence of  $S$  is described by equation (2) [19]. Figure 5 shows the two-band model fits for thermopower using equation (2). The parameters  $1/\sigma_{01}$ ,  $a$  and  $1/\sigma_{02}$  are taken from table 1. The activation gap  $E_{gS}$  is taken as a variable while fitting. The values  $A$ ,  $C$ ,  $E_{gS}$  are tabulated in table 1. The term  $A$  decreases as Al concentration increases due to an increase in the carrier concentration. The values reach  $dS/dT$  in the zero temperature limit for metals far from the MI transition. The activation gaps estimated from resistivity and thermopower are in good agreement with each other. However, the values are higher

than those estimated from simple activation behavior alone at high temperatures [11, 12]. This is due to the removal of electronic states at the band edges and the appearance of states at the Fermi level when carriers are doped. Hence, at low concentration of Al, where the states at the Fermi level are localized, the effective gap estimated from the two-band model has a larger value.

## 5. Conclusion

The conductivity in metals near MI transitions has two contributions. At low temperatures, the conductivity is dominated by the impurity band leading to a positive coefficient of resistivity and a linear temperature dependence of thermopower. At high temperatures, the activated carriers dominate the conductivity with an exponential and inverse temperature dependence of resistivity and thermopower respectively. A parallel-resistor model can be used to describe the temperature dependence of resistivity and thermopower of such systems.

## Acknowledgments

The authors thank Dr P Chaddah and Professor Ajay Gupta for their support and encouragement. The authors would also like to thank Professor R Srinivasan, Dr B A Dasannacharya, and Professor V N Bhoraskar for their encouragement. One of the authors (LSSC) would like to thank CSIR for financial support.

## References

- [1] Jaccarino V, Wertheim G K, Wernick J H, Walker L R and Sigurds Aarj 1967 *Phys. Rev.* **160** 476
- [2] Tajima K, Endoh Y, Fischer J E and Shirane G 1988 *Phys. Rev. B* **38** 6954
- [3] Castor Fu and Doniach S 1995 *Phys. Rev. B* **51** 17439
- [4] Wachter P and Travaglini G 1985 *J. Magn. Magn. Mater.* **47/48** 423
- [5] Anisimov V I, Ezhov S Y, Elfimov I S, Solovyev I V and Rice T M 1996 *Phys. Rev. Lett.* **76** 1735
- [6] Sales B C, Jones E C, Chakoumakos B C, Fernandez-Baca J A, Harmon H E, Sharp J W and Volckmann E H 1994 *Phys. Rev. B* **50** 8207
- [7] Chernikov M A, Degiorgi L, Felder E, Paschen S, Bianchi A D, Ott H R, Sarrao J L, Fisk Z and Mandrus D 1997 *Phys. Rev. B* **56** 1366
- [8] Bauer E, Galatanu A, Hauser R, Reichl Ch, Wiesinger G, Zaussinger G, Galli M and Marabelli F 1998 *J. Magn. Magn. Mater.* **177–181** 1401
- [9] Mani A, Bharathi A, Mathi Jaya S, Reddy G L N, Sundar C S and Hariharan Y 2002 *Phys. Rev. B* **65** 245206
- [10] Yeo S, Nakatsuji S, Bianchi A D, Schlottmann P, Fisk Z, Balicas L, Stampe P A and Kennedy R J 2003 *Phys. Rev. Lett.* **91** 046401
- [11] DiTusa J F, Friemelt K, Bucher E, Aeppli G and Ramirez A P 1997 *Phys. Rev. Lett.* **78** 2831
- [12] DiTusa J F, Friemelt K, Bucher E, Aeppli G and Ramirez A P 1998 *Phys. Rev. B* **58** 10288
- [13] Chapman P W, Tufte O N, David Zook J and Long D 1963 *J. Appl. Phys.* **34** 3291
- [14] Xin Y, Wong K W, Fan C X, Sheng Z Z and Chan F T 1993 *Phys. Rev. B* **48** 557
- [15] Mason T A, Aeppli G, Ramirez A P, Clausen H N, Broholm C, Stucheli N, Bucher E and Palstra T T M 1992 *Phys. Rev. Lett.* **69** 490
- [16] Glushkov V V, Sluchanko N E, Demishev S V, Kondrin M V, Pronin A A, Petukhov K M, Bruyseraede Y, Moshehalkov V V and Menovsky A A 2000 *Physica B* **284–288** 1179
- [17] Herring C 1954 *Phys. Rev.* **96** 1163
- [18] Barnard R D 1972 *Thermoelectricity in Metals and Alloys* (London: Taylor and Francis)
- [19] Geballe T H and Hull G W 1955 *Phys. Rev.* **98** 940